International Journal of Modern Manufacturing Technologies
ISSN 2067–3604, Vol. XIV, No. 3 / 2022
https://doi.org/ 10.54684/ijmmt.2022.14.3.21

RESEARCH ON THE COMPRESSIVE BEHAVIOUR OF CERAMIC COMPOSITE MATERIAL BASED ON BENTONITE

Sorin Butuc (Anghel), Simona Matei, Maria Stoicanescu

Transilvania University of Brasov, Material Science Department, 29 Eroilor Blvd, 500036, Brasov, Romania

Corresponding author: Maria Stoicanescu, stoican.m@unitbv.ro

Abstract: The paper presents the results of a study on the compressive behaviour of ceramic composite made with bentonite matrix. During the study, samples were made of ceramic composite, of filter type, cylindrical with a diameter of 16 mm and heights between 14-16 mm. To achieve the porous structure, the matrix was reinforced with ceramic powders of Al_2O_3 and SiC, and to control the pore size, metal powders of Al and Fe were used in percentages between 3-12%. The compaction of the samples thus obtain was performed by mechanical pressing in a metal mould on a universal testing machine with a force F=20 kN. In order to test them in compression, the samples were sintered in an oven at T=1100°C in a heat treatment oven after a predetermined treatment cycle. For each test, the diagram was registered with the help of the software from the machine's equipment, respectively the behaviour of the different sintered ceramic composite samples. The results thus obtained were analysed in correlation with the composition of the tested samples. In conclusion, dependencies were established between the type, nature and ratio of the constituent samples of ceramic composite and their behaviour at the request of compression.

Key words: ceramic composite, bentonite, compressive behaviour, uniaxial compression test, sintering process.

1. INTRODUCTION

Industrial development and urban expansion have significantly contributed to the increase in pollution. For reasons related to reducing pollution, there is a high interest in the use of ecological, non-polluting resources. The design of new, ecological materials, with minimal impact on the environment, is a necessity. Ceramic materials have responded to this need and, therefore, they have been studied and applied in various fields. Otitoju et al. (Tumise et al., 2020). indicate that the properties of the material, sintering temperature and pressure, influence the grain size and the porosity of the ceramic which have an explicit effect on the mechanical strength and corrosion resistance of the ceramic components. Otitoju et al. (Tumise et al., 2020) refers to advanced ceramics as high performance ceramics, with a rigorously controlled and manufactured composition, with detailed regulations from refined raw materials and characterised by precisely specified properties. The main control parameter of the reaction in most synthesis pathways is temperature, because it has an exponential effect (Tumise et al., 2020).

The sintering process takes place by bonding the particles upon heating by mass transfer and surface transport mechanisms with the main purpose of obtaining a dense solid component, (Tumise et al., 2020).

Sintering is correlated with several factors such as: sintering temperature and time, raw material density, agglomerations, pressure, heating rate, cooling rate, sintering atmosphere, grain size, porosity, (Tumise et al., 2020).

The design of filters made of ceramic composite materials to be used in a process of filtering drinking water involves knowledge of the structural aspects in correlation with the properties of the materials when subjected to mechanical stresses. Mustafa et al. (Mustaphaa et al. 2021) considers that the filtration method by using ceramic filters is a simple and economical method for water treatment. For this, the filters must be effective. Mustapha considers that the effectiveness of a filter in the filtration process depends on the filtration environment, porosity, composition and quality of the filter (Mustaphaa et al. 2021).

In order to respond to this problem, ceramic filters must be tested.

Samples of ceramic composites were subjected to the uniaxial compression test. Meille S. (Meille, 2021) indicates that the uniaxial compression test must be a uniform stress in the sample, and, for this purpose, the contact areas between the upper and lower surfaces between the sample and the contact plates of the testing machine have to be parallel.

Meille (Meille, 2021) considers that a possible non-parallelism or an imperfect parallelism between the

upper and lower surfaces of the sample, as well as the surface roughness, can lead to stress concentrations which generate irreversible local damage, thus leading to a nonlinear behaviour on the load-deflection curve. Stojanovic et al. (Stajamovic and Glisovic, 2021) indicates that the improvement in hardness properties of ceramic materials is due to the relationship between crack progression and the dispersion of composite particles.

Krimsky et al. (Krimsky et al, 2019. Hogan et al. 2016) emphasises that internal cracks have a considerable effect on the response of the composite material.

Previous studies on ceramic materials have focused on the fact that the size, shape, type of microstructural features that represent the premises of the fracture initiation points have been characterised (Krimsky et al, 2019. Hogan et al. 2016. Xie et al., 2016. Powell, Heuer, 1990. Danzer, 2014.Hogan et al. 2016). Under quasi-static compression, the defects in the material are activated first and they lead to an increase in cracks in the sample (Hogan et al., 2016. Matei, 2019).

Danzer (Danzer, 2014) specifies that the strength of materials, the strength of samples and the strength of components are often quite different properties.

Moreover, in order to avoid any unexpected damage to the components, the internal stresses, the quality of the surfaces and the correct handling of the ceramic materials and components must be taken into account.

The ceramic matrix contains bentonite, silicon carbide, alumina (Matei et al., 2019). The term bentonite refers to a very plastic inflatable clay belonging to the group of spectate minerals, deriving from the in situ alteration of volcanic ash and tuff (Barbieri et al., 2020). Montmorillonite is the best known smectite clay, and its structural formula is $M+ynH_2O(Al_2yMgy)Si_4O_{10}(OH)_2$ (Barberi et al., 2020).

The use of bentonite is a viable and environmentally friendly solution (Barberi et al., 2020, Spauding, 2008). The use of bentonite in the composite matrix requires a knowledge of the structure and of the temperature dependent on behaviour. Ceramic samples support a high level of applied loads (Tunmise et al., 2020. Barberi et al., 2020).

The strength calculation involves determining a ratio between the breaking strength and the cross-sectional area of the sample. In the case of mechanical compression stress, the friction between the plates of the testing machine and the sample surfaces generating local stresses in the sample is also taken into account.

The aim of the paper is to study the behaviour of samples consisting of ceramic composite materials alloyed with metallic particles in different percentages when subjected to the mechanical compression stress and the influence thereof on the breaking strength.

2. MATERIALS USED AND PROCEDURE

2.1. Materials used

Two matrices based on bentonite powder (53% montmorillonite $(Na,Ca)_{0.33}(Al,Mg)_2(Si_4O_{10})(OH)_2nH_2O$; 1.3% Fe_2O_3; 45.7% SiO_2) were used to obtain the composite materials. The first composite matrix was made of bentonite powder mixed with SiC ceramic powder of 60-80 μm grain size, and the second composite matrix was made of bentonite powder mixed with Al_2O_3 ceramic powder of 50 μm grain size. For their differentiation and for a good analysis, the compounds based on bentonite mixed with SiC particles were marked by S, and those based on bentonite mixed with particles of Al_2O_3 were marked by P. The chemical composition and properties of bentonite are shown in table 1 (Matei et al. 2019. Lee et al. 2019. Matei et al., 2019. Matei and Crisan, 2019).

Table 1. The composition and properties of bentonite (Matei et al. 2019. Lee et al. 2019. Matei et al., 2019. Matei and Crisan, 2019).

Fine sand [%]	1.39
Dust [%]	20.18
Clay [%]	78.43
Specific weight [g/cm^3]	2.77
Yield strength [%]	393
Plastic limit [%]	50
Shrinkage limit [%]	18
Specific surface area [m^2/g]	495

The bentonite powder provides good absorption properties, while SiC and Al_2O_3 ceramic powders give the composite a porous structure.

The bentonite matrix mixed with SiC was made in a proportion of 40/60 percent. Similarly, the bentonite matrix mixed with Al_2O_3 was made in a proportion of 40/60 percent.

The composition of S and P-type composites are indicated in table 2:

Table 2. Composition of S and P-type composites.

Composite type	Bentonite		Al_2O_3		SiC	
	[%]	Weight [g]	[%]	Weight [g]	[%]	Weight [g]
S	40	24	-	-	60	36
P	40	24	60	36	-	-

Metallic particles of Al and Fe were added in proportions of 3, 6, 9, 12% to the matrices of the composites thus obtained.
Metallic particles were added to control the pore size of the composite material.
There was studied their effect on the compression strength of the composites obtained.
The grain size of the Al particles used is < 75 μm and for the Fe particles is < 100 μm.
There were obtained several groups of composite materials by adding metallic particles to the structure of the composite, and they were named according to the nature of the composite matrix and the amount of metallic particles added to the structure.
Thus, if the composite has a matrix consisting of bentonite with ceramic particles of SiC to which was added an amount of 3%, 6%, 9%, respectively 12% metallic particles of Al or Fe, the name of the composite is S-3Al (Fe), S-6Al (Fe), S-9Al (Fe), S 12Al (Fe).
The composition of the materials thus obtained is presented in table 3.
Similarly, the composites with a bentonite matrix with Al2O3 ceramic particles to which an amount of 3%, 6%, 9%, respectively 12% metallic particles of Al or Fe was added have been named as follows: P-3Al (Fe), P-6Al (Fe), P-9Al (Fe), P-12Al (Fe).

Table 3. S-type composites with Al and Fe particles.

Composite type	Bentonite		SiC		Al		Fe	
	[%]	Weight [g]	[%]	Weight [g]	[%]	Weight [g]	[%]	Weight [g]
S-3Al	38.10	24	57.14	36	4.76	3	-	-
S-6Al	36.37	24	54.54	36	9.09	6	-	-
S-9Al	34.78	24	52.18	36	13.04	9	-	-
S-12Al	33.33	24	50.00	36	16.67	12	-	-
S-3Fe	38.10	24	57.14	36	-	-	4.76	3
S-6Fe	36.37	24	54.54	36	-	-	9.09	6
S-9Fe	34.78	24	52.18	36	-	-	13.04	9
S-12Fe	33.33	24	50.00	36	-	-	16.67	12

Table 4. P-type composites with Al and Fe particles.

Composite type	Bentonite		Al_2O_3		Al		Fe	
	[%]	Weight [g]	[%]	Weight [g]	[%]	Weight [g]	[%]	Weight [g]
P-3Al	38.10	24	57.14	36	4.76	3	-	-
P-6Al	36.37	24	54.54	36	9.09	6	-	-
P-9Al	34.78	24	52.18	36	13.04	9	-	-
P-12Al	33.33	24	50.00	36	16.67	12	-	-
P-3Fe	38.10	24	57.14	36	-	-	4.76	3
P-6Fe	36.37	24	54.54	36	-	-	9.09	6
P-9Fe	34.78	24	52.18	36	-	-	13.04	9
P-12Fe	33.33	24	50.00	36	-	-	16.67	12

The composition of the materials thus obtained is presented in table 4.

2.2. Procedure

The matrix based on bentonite mixed with SiC, named S, was obtained by dry mixing in a container for 15 minutes a mass of 24 g bentonite with 36 g ceramic particles of SiC, resulting in a proportion of 40/60 percent. The matrix based on bentonite mixed with Al_2O_3, named P, was obtained by dry mixing in another container for 15 minutes a mass of 24 g bentonite with 36 g ceramic particles of Al_2O_3, resulting in a proportion of 40/60 percent. An amount of 7.2% distilled water was introduced into the matrix obtained, accounting for

a total of 12% per 100 g of mixture. The mixing of the material was continued and, in the moistened material obtained, additional amounts of metallic particles of Al and Fe were introduced in percentages between 3% and 12%, and it was mixed until fully homogenized. There were obtained several groups of materials. The prepared material, in wet state, was compacted at a force F= 20 kN in a metal mould with the help of the universal testing machine, type WDW-150S. Following compaction, there were obtained cylindrical samples of material with a diameter of Ø =16 mm and a height h between 14 and 16 mm. Several samples subsequently used in the study were obtained from each type of composite. The software of the universal testing machine recorded the compaction diagrams for the samples obtained. The samples were left to dry for 48 hours at room temperature between T = 20-23 °C. After drying, the samples were sintered [19] at a temperature of T= 1100 °C under normal atmosphere in a Nabertherm heat treatment furnace following a heat treatment cycle. Thus, the heating rate was preset to a value of vi =15 °C/min. The heat treatment cycle involved heating from the temperature T = 40 °C - 1100 °C for 71 minutes, holding at T =1100 °C for 30 min, followed by cooling from T = 1100 °C- 40 °C for 90 minutes. The sintering diagram is presented in figure 1.

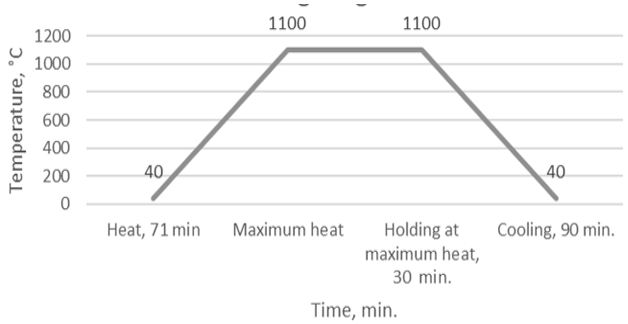

Fig. 1. Sintering diagram.

There were obtained monolithic cylindrical samples, which were subjected to compression. Similar research on testing cylindrical compression samples was performed previously (Craig et al., 2015. Manassero et al, 2020). The compression test of the cylindrical specimens was conducted using the universal testing machine type WDW-150S by applying a force F = 20 kN. This machine allows the performance of tests at forces between 1 and 150 kN to study the behaviour of the samples at mechanical stresses of traction, compression, bending at temperatures between -120 °C and 1200 °C. The machine is equipped with a software that controls the functional parameters, allowing the recording of test results in the form of stress-strain diagrams. For the study performed, compression tests were performed on the ceramic composite samples. The test was performed in a normal atmosphere, at room temperature.

3. EXPERIMENTAL PROCEDURE

3.1. Composites based on bentonite, silicon carbide and aluminum (S-Al)

The results of the tests performed represent the average of three tests performed on the same type of material. These results are shown in table 5 and figure 2.

Figure 2 shows that the compression strength decreases when metallic particles of Al are added to the basic matrix in a first phase. This is due to the fact that by oxidising the metallic particles during sintering (conducted in normal atmosphere), the resulting oxides manifest themselves as areas of disruption of the bonds inside the material.

Table 5. Compression test results for the S-Al samples.

Composite type	Maximum force, Fbc [kN]	Compression strength, Rbc [Mpa]
S	16.55	82.5
S-3Al	12.51	64
S-6Al	15.76	78.5
S-9Al	19.93	100
S-12Al	32.76	163

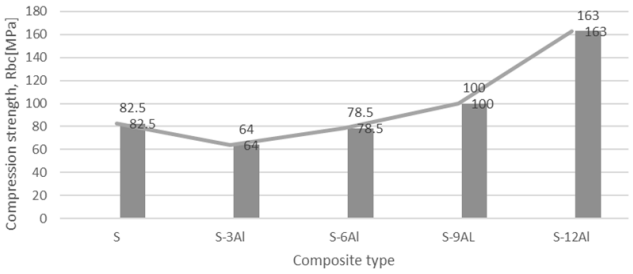

Fig. 2. Diagram of the average values of the results of the tests conducted on S-Al type materials.

The increase of the percentage of Al particles in the composite determines the increase of the amount of aluminum oxide formed during sintering, accompanied by an increase in volume around these particles, thus leading to the occurrence of certain internal compression stresses. These stresses are partially relaxed by compacting the material (reducing the pore size) and, on the other hand, they can remain as residual stresses favoring the increase of the compression strength of the material.

3.2. Composites based on bentonite, silicon carbide and iron (S-Fe)

The results of the tests performed represent the average of three tests performed on the same type of material. These results are shown in table 6 and figure 3.

When adding Fe particles to the composite, there is found an influence similar to that of Al up to an addition of 6% Fe. Above these values, the compression strength of the material begins to decrease quite sharply.
This effect can be determined, on the one hand, by the generation of internal cracks upon local volume increases following the oxidation of Fe particles during sintering and, on the other hand, by the interactions between the Fe and SiC oxides in the composite.

Table 6. Compression test results for the S-Fe samples.

Composite type	Maximum force, Fbc [kN]	Compression strength, Rbc [Mpa]
S	16.55	82.5
S-3Fe	13.63	68
S-6Fe	18.46	92
S-9Fe	13.13	65
S-12Fe	11.49	57.5

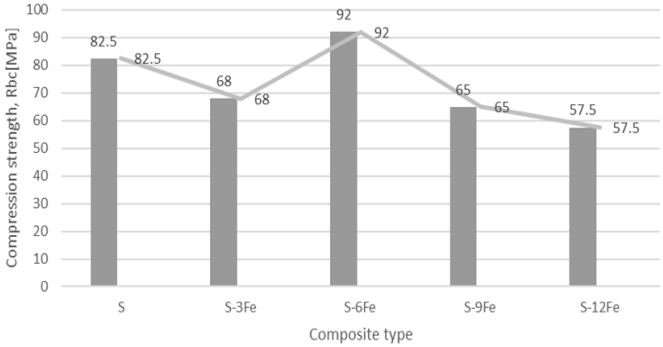

Fig. 3. Diagram of the average values of the results of the tests conducted on S-Fe type materials.

3.3. Composites based on bentonite, alumina and aluminium (P-Al)

The results of the tests performed represent the average of three tests performed on the same type of material. These results are shown in table 7 and figure 4.
When Al particles are added to P-type composites (with Al_2O_3 ceramic particles), the effects are similar to those in the case of the S-type composites (with SiC ceramic particles). However, there are quite important differences in terms of quantity.

Table 7. Compression test results for P-Al samples.

Composite type	Maximum force, Fbc [kN]	Compression strength, Rbc [MPa]
P	20.88	103.5
P-3Al	16.13	83
P-6Al	21.83	108.5
P-9Al	22.05	111
P-12Al	22.83	115

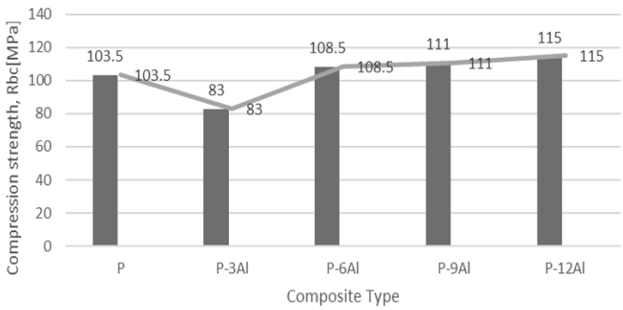

Fig. 4. Diagram of the average values of the results of the tests conducted on P-Al type materials.

When Al particles are added to P-type composites (with Al_2O_3 ceramic particles), the effects are similar to those in the case of the S-type composites (with SiC ceramic particles). However, there are quite important differences in terms of quantity. After a comparable reduction of the compression strength in the two situations, up to 3% Al, the increase of the compression strength with the increase of the percentage of Al is much lower in the case of P-type composites than in the case of S-type composites (compare figure 4 to figure 2).

3.4. Composites based on bentonite, alumina and iron (P-Fe)

The results of the tests performed represent the average of three tests performed on the same type of material. These results are shown in table 8 and figure 5.

Table 8. Compression test results for the P-Fe samples.

Composite type	Maximum force, Fbc [kN]	Compression strength, Rbc [MPa]
P	20.88	103.5
P-3Fe	15.51	77
P-6Fe	22.80	113.5
P-9Fe	27.42	127.5
P-12Fe	28.82	143.5

The addition of Fe particles to P-type composites (with Al2O3 ceramic particles) has a different influence than that on the S-type composites (with SiC ceramic particles), very obvious at contents of over 6% Fe (compare figure 5 to figure 3). This is due to the way in which the Fe oxides formed during sintering interact with the components of the matrix. In the P-type composites, the Fe oxides do not interact practically with the components of the matrix, generating at their formation internal stresses that ensure the compaction of the material and the increase of the compression strength.

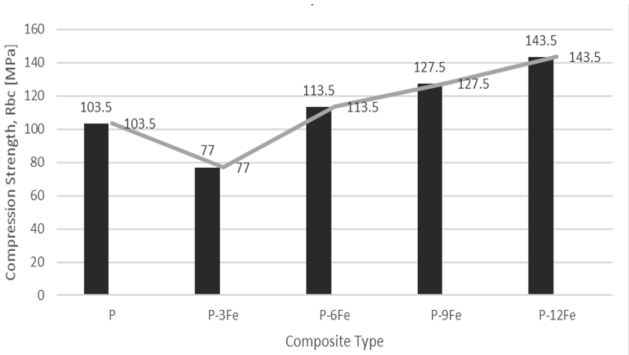

Fig. 5. Diagram of the average values of the results of the tests conducted on P-Fe type materials.

In S-type composites, Fe oxides interact mainly with SiC, generating reaction products that can reduce the internal bonds in the composite, reducing its compression strength.

4. CONCLUSIONS

The following conclusions can be drawn from the research carried out:

– The addition of metallic particles to the studied composites determines, for low values of the additions (up to 3%), the reduction of their compression strength. The reason is the formation of oxides of the respective metals during the sintering of the composites in the atmosphere, accompanied by local increases in volume, the occurrence of local compression stresses and if interruptions of intergranular bonds;

– As the amount of metallic particles increases, the importance of the local compression stresses generated by the formation of metal oxides also increases. These cause the material to compact and increase its compression strength, as long as they do not produce internal cracks (if their value becomes greater than the specific strength of the material);

– In addition to the compaction effect of the material, the metal oxides formed during sintering influence the compression strength depending on the interaction with the granular materials in the composite The more active these interactions (the case of the Fe oxides in the composite with SiC particles) the stronger the compression strength of the composite.

5. REFERENCES

1. Tunmise, A., Otitojua, P., Ugochukwu, O., Guanting, C., Yang, L., Martin, O.O., Sanxi, L., (2020). J. of Ind. and Eng. Ch., 87, 34-65.
2. Mustaphaa, S., Oladejoa, T.J., Muhammeda, N.M., Saka, A.A., Oluwabunmi, A.A., Abdulkabir, M., Omotunde, O., (2021)., Sci. Afr., 11, e00705.
3. Meille, S., (2021). Encycl. of Mat. 1, pp. 745-761.
4. Stojanovic, B., Glisovic, J., (2021). Encycl. of Mat., 2, 275-292.
5. Krimsky, E., Ramesha, K.T., Bratcherc, M., Fosterc, K.T., Hogand, J.D. (2019). Adv. Cer.Eng., 208, 107-118.
6. Hogan, J.D., Farbaniec, L., Shaeffer, M., Ramesh, K.T., (2015). J. Am. Cer. Soc., 98(3), pp. 902-912.
7. Hogan, J. D., Farbaniec, L., Sano, T., Shaeffer, M., Ramesh, K. T., (2016). Act. Material, 102, 263-272.
8. Xie, K.Y., Kulwekar, K., Haber, R.A., LaSalvia, J. C., Hemker, K.J., (2016). J. Am Cer Soc., 99(8), 2834-2841.
9. Powell, C.A., Heuer, A.H., (1990). J. Am Cer Soc.,73(12), 3670-3676.
10. Danzer, R., (2014). J. of the Eur. Cer. Soc., 34, 3435-3460.
11. Hogan, J.D., Farbaniec, L., Sano, T., Shaeffer, M., Ramesh, K.T., (2016). Act. Mater., 102, 263-272.
12. Matei, S., Varga, B., Bedo, T., Pop. M.A., Stoicanescu, M., Crisan, A., (2019). Mat. Today: Proc.1, 1041-1050.
13. Wessel, R., Koch, C., Gabbiani, F., (1996). C*oding of time-varying electric field amplitude modulations in a wave-type electric fish*, J. Neurophysiol., 75(6), 2280–93.
14. Spaulding, C., Masse, F., LaBrozzi, J., (2008). Civ. Eng. Mag., 78(4), 54-59.
15. Matei, S., Crisan, A., (2020). Compozite Termoplastice. Compozite Termorezistente EUT-BV, pp. 55, 87.
16. Lee, H., Rukmanikrishnan, B., Lee, J., (2019). Int.Jour. of Biolog. Macr., 141, 538–544.
17. Matei, S., Varga, B., Bedo, T., Pop, M.A., Stoicanescu, M., Crisan, A., (2019). Mat Today: Proc. 19, 1041-1050.
18. Matei, S., Crisan, A., (2019). Bul. of the Trans. Univ., 12, 19-26.
19. Choi, H.J., Kim, J.U., Kim, H.S., Kim, K.H., Lee, M.H., (2015). Cer. Int., 41, 10030-10037.
20. Craig, B.H., Zhai, H., Wang, X., (1994). J. of Geo. Engin., 120, 366-387.
21. Manassero, M., Benson, C.H., Bouazza, A. (2000). Inter. Sympos ISRM., Melbourne, ISRM-IS-2000-012.

Received: April 13, 2022 / Accepted: December 15, 2022 / Paper available online: December 20, 2022